The Planetary Science Journal, 2:66 (13pp), 2021 April https://doi.org/10.3847/PSJ/abeaa0

Ina Lunar Irregular Mare Patch Mission Concepts: Distinguishing between Ancient and Modern Volcanism Models

Le Qiao[1], James W. Head[2], Lionel Wilson[3], and Zongcheng Ling[1]
[1] Shandong Key Laboratory of Optical Astronomy and Solar-Terrestrial Environment, School of Space Science and Physics, Institute of Space Sciences, Shandong University, Weihai, Shandong, 264209, People's Republic of China; leqiao.geo@gmail.com
[2] Department of Earth, Environmental and Planetary Sciences, Brown University, Providence, RI 02912, USA
[3] Lancaster Environment Centre, Lancaster University, Lancaster LA1 4YQ, UK
Received 2020 October 24; revised 2021 January 24; accepted 2021 February 25; published 2021 April 6

Abstract

The Ina irregular mare patch, an ∼2 × 3 km summit depression on an ancient ∼22 km diameter shield volcano, displays two very enigmatic units: (1) dozens of dark convex-upward mounds and (2) a very rough, optically immature floor unit with very sharp morphologic contacts between the two. Controversy surrounds the age interpretation of Ina; superposed impact crater size–frequency distributions (CSFDs) suggest an age of ∼33 Ma, consistent with the presence of sharp contacts between the units and indicating that mare volcanism continues to today. Models of the terminal stages of volcano summit pit crater activity suggest an age coincident with the building of the shield, ∼3.5 Ga; these models interpret the CSFD age and sharp contacts to be due to an extremely porous lava lake floor and extrusion and solidification of magmatic foams. We present robotic–human exploration mission concepts designed to resolve this critical issue for lunar thermal evolution.

Unified Astronomy Thesaurus concepts: Lunar features (953); Lunar evolution (952); Lunar maria (961); Lunar surface (974); Volcanoes (1780); Planetary structure (1256)

1. Introduction and Background

While examining the high-resolution orbital photographs taken by the Apollo 15 crew in 1971 August, Whitaker (1972) noted a very unusual and enigmatic depression feature (18.66°N, 5.30°E), ∼3 × 2 km in size, with about half of the depression floor covered with blobs of mare materials with an appearance similar to "dirty mercury." Located in a small mare in the central portion of the nearside Moon, the feature was informally named "D-Caldera" (Cernan et al. 1972; El-Baz 1973; Evans & El-Baz 1973) and then formally known as Ina (Defense Mapping Agency 1974; Strain & El-Baz 1980; Figures 1 and 2). Its peculiar shape and interior structures intrigued many Apollo program scientists (El-Baz 1972, 1973; Whitaker 1972). Soon after its discovery, a special orbital visual observation effort for the Ina feature was planned during the Apollo 17 mission in 1972 December. Command Module Pilot (CMP) Ronald E. Evans then presented remarkable observations of the Ina/D-Caldera feature from lunar orbit (Cernan et al. 1972):

"[The] D-Caldera is sure a depression. Like nothing I have ever seen before … At this point, you get a dark tan, a mare-type material. And then it is a light gray down in the D-Caldera itself… And then it has got bumps that stick up, and the bumps themselves are the light tan material… And down between the bumps [is] a rough, blocky, gray material." (CMP, revolution 28; words in brackets are not original)

"The pictures confirm a topographic rise around the D-Caldera, just a slight one, and it is about half the width of the D-[Caldera]. And it seems to be a raised, flat rim around it. The color of the raised bumps down in the D-Caldera are the same as the surrounding material. The bumps that are raised up are smooth looking and … the part of the depression, anyhow, is a light bluish gray." (CMP, revolution 36)

"Down in the caldera, the gray blocky-type of stuff [looks like] water drops on a surface … But it would leave a depression due to a surface tension … And then you have little bubbles that float across there … I could not see a light-colored annulus [around D-Caldera] … There is nothing surrounding D-Caldera that looks like the silver, gray material that has depressed. The little bumps in D-Caldera are the same color and the same smoothness as the mare material surrounding the area." (CMD, revolution 40)

In addition, the Apollo 17 mission also obtained a sequence of orbital photographs with both color and black-and-white film. Many Apollo 17 photographs were taken in very low Sun illumination conditions, which exaggerated surface object shadow patterns and thus significantly enhanced surface morphologic detectability. Geological investigations of these photographs identified Ina as a summit vent depression atop a small extrusive lava dome with a raised rim "collar" feature (El-Baz 1973; Evans & El-Baz 1973; Strain & El-Baz 1980; Figure 1). The interior of Ina is characterized by various terrain types, including (1) dozens of disconnected blister-like smooth textured mounds; (2) a hummocky-textured floor unit, which is further divided into two albedo portions, light-colored and dark-colored (the latter occurs predominantly along the eastern edge of the Ina floor); and (3) bright materials found around the raised mounds and along the edges of the floor (Figure 2). On the basis of these observations and comparison with terrestrial volcanic analogs (for instance, lava pillars in northern Iceland at Dimmuborgir; Strain & El-Baz 1980), most or all of the morphologies associated with Ina were described as being volcanic in origin (El-Baz 1972, 1973; Evans & El-Baz 1973; Strain & El-Baz 1980). Specifically, the hummocky floor terrains were interpreted as solidified lava lake crust and pyroclastic deposits, and the mounds were thought to be formed as discrete lava extrusions, among the youngest volcanic

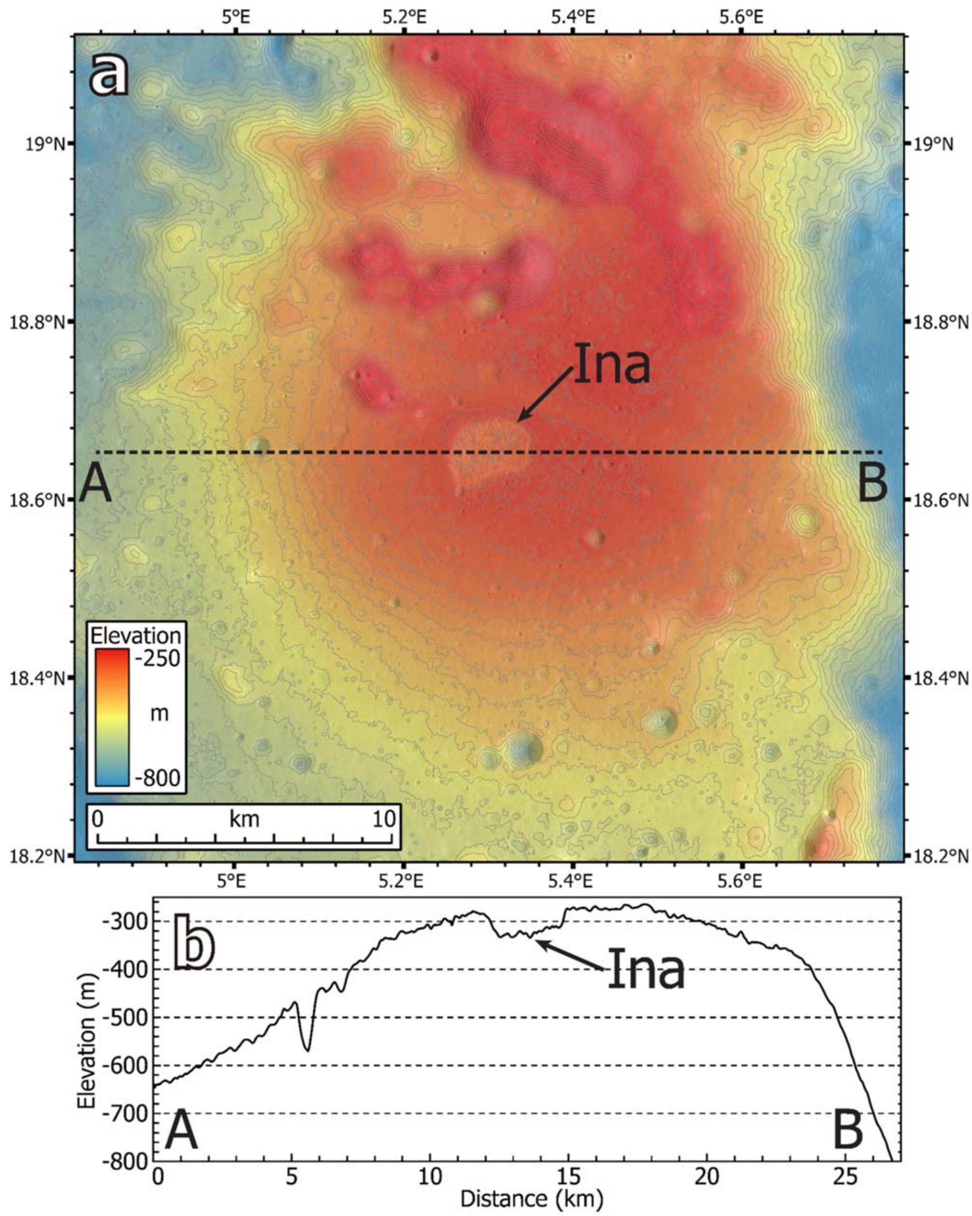

Figure 1. Location and general setting of the Ina pit crater. (a) SLDEM2015 topography of the mare surface surrounding Ina, overlaid on Kaguya TC evening mosaic, 25 m contour interval, and (b) a west–east (A–B) topographic profile across the Ina shield and summit pit crater, derived from SLDEM2015 topography.

features on the Moon (El-Baz 1972, 1973; Evans & El-Baz 1973; Strain & El-Baz 1980).

The international fleet of spacecraft launched to the Moon during the past decade has obtained unprecedented high-resolution imagery data for the nearly global lunar surface, especially the Lunar Reconnaissance Orbiter Narrow Angle Cameras (LROC NAC) on board NASA's Lunar Reconnaissance Orbiter, which has continuously mapped the lunar surface with a pixel size of ~0.5–2 m (from the nominal 50 km orbit) since 2009 (Robinson et al. 2010). Survey of the LROC NAC imagery sets found many lunar surface features resembling Ina (Stooke 2012; Braden et al. 2014; Zhang et al. 2018). In particular, Braden et al. (2014) conducted a global search of NAC data and cataloged a total of 70 small mare features with Ina-like characteristics, which they termed irregular mare patches (IMPs). Integrating analyses from the morphology, topography, stratigraphy, and spectroscopy of Ina and other IMP features led Braden et al. (2014) to suggest that the lower hummocky terrains are a collapsed volcanic caldera floor or fragmented lava lake crust, and the stratigraphically higher mounds are terminal-stage lava extrusions (Figure 3). Braden et al. (2014) also investigated the size–frequency distribution of impact craters (CSFD) superposed on the mound terrains at the three largest IMPs (Ina, Sosigenes, and Cauchy 5) and found that they were all younger than 100 Ma. These ages implied a significant prolongation of the lifetime of lunar volcanism from the youngest previously established ~1 Ga ago (e.g., Hiesinger et al. 2011; Morota et al. 2011) to geologically very recent, which, if confirmed, would raise a host of questions concerning the correctness of current models of lunar thermal and magmatic evolution (e.g., Head & Wilson 1992; Shearer et al. 2006; Ziethe et al. 2009).

In addition to the geologically very recent volcanic eruption model, various alternative scenarios to account for the characteristics, age, and origin of Ina/IMPs have been introduced (Table 1). These include the following.

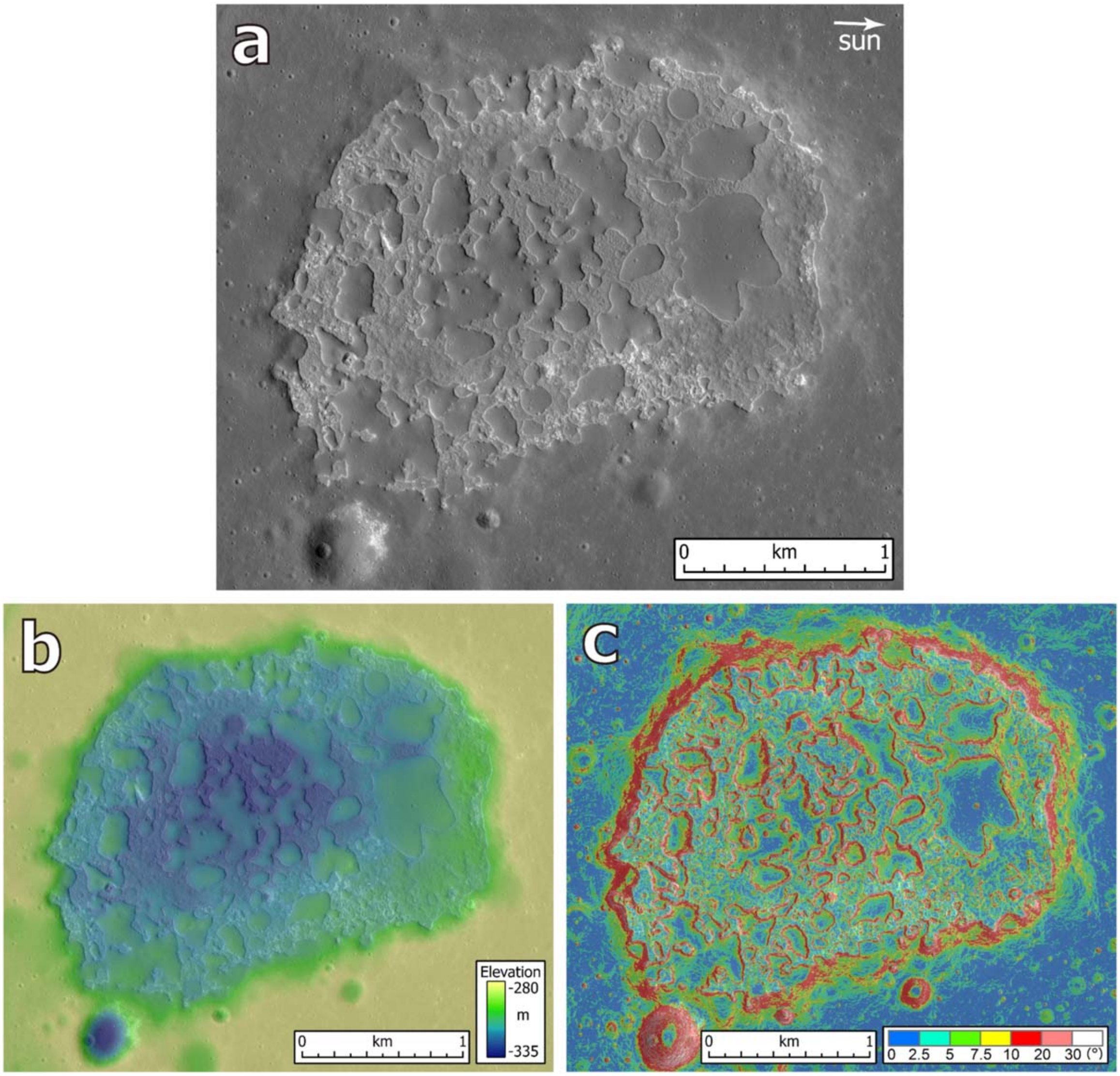

Figure 2. Ina interior imagery, topographic and slope maps. (a) LROC NAC image (frame M119815703, 0.48 m pixel^{-1}, ∼56° incidence angle), (b) LROC NAC DTM topography (2 m pixel^{-1}) overlaid on NAC image M119815703, and (c) NAC DTM-derived slope (6 m baseline) map overlaid on LROC NAC M119815703. The solar illumination direction is indicated by the white arrow in panel (a).

(1) Sublimation-induced high reflectance of the floor terrains (Whitaker 1972).

(2) Exposure of underlying ancient (>3.5 Ga) mare deposits through the removal of the surface regolith layer by sudden outgassing of deep juvenile volatiles within the past 10 Ma (Schultz et al. 2006).

(3) Lava flow inflation (mounds) and subsequent lava breakout (floor hummocky terrains; Garry et al. 2012).

(4) Explosive volcanic eruptions and the resultant deposition of fine-grained, block-free pyroclastics. Carter et al. (2013; note that this model is proposed for the Cauchy 5 IMP occurrence, one of the three dated young IMPs (∼58 Ma; Braden et al. 2014), but not specifically for Ina). A compilation of these previously proposed scenarios and the resultant deposits for lunar IMPs can be found in Qiao et al. (2020a), and an evaluation of some of these models was presented in Qiao et al. (2018).

(5) Formation of Ina in the terminal stages of the associated ancient shield volcano, with the unusual characteristics and age attributed to late-stage, magmatic volatile-rich lava lake activity and the resulting macro- and microvesicular substrate properties (Qiao et al. 2017, 2018, 2019, 2020a, 2020b).

Following the comprehensive initial work by Braden et al. (2014), an updated catalog of the entire IMP population was compiled, and comprehensive geological analyses of several representative IMPs including Ina were undertaken by Qiao et al. (2017, 2018, 2019, 2020a, 2020b). This provided more detail to this interpretation for the emplacement mechanism and age of Ina and other lunar IMPs. Qiao et al. (2020a) presented an updated inventory of 91 IMP occurrences by synthesizing previous IMP identification results. By documenting the detailed geological context information for each cataloged IMP feature, Qiao et al. (2020a) found that the modes of occurrence of the population of lunar IMPs could be classified into two major groups: (1) pit crater environments (or closed environments), in which the IMPs are contained within volcanic pits, for instance, the summit calderas of small shield volcanoes, volcanic dike-tip rilles, or endogenetic pit crater chains; and (2) mare flow environments (or open environments), in which the IMPs are simply emplaced on typical

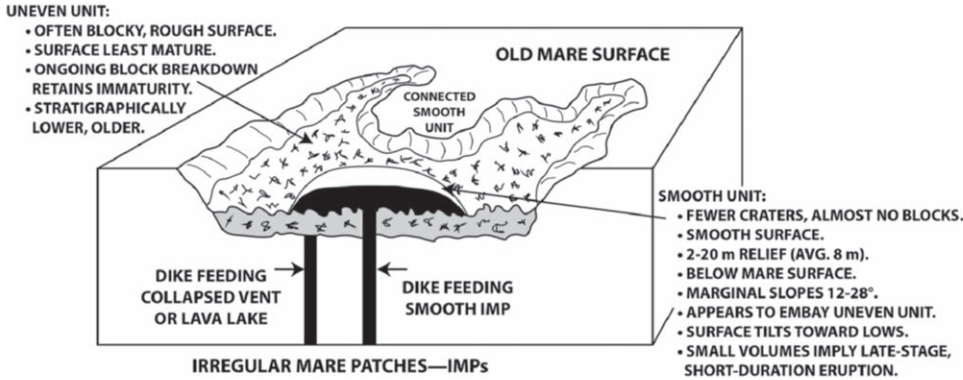

Figure 3. Block diagram for the major structures and characteristics of the Ina pit crater and their mode of emplacement as interpreted by Braden et al. (2014), in which the uneven floor units represent fragmented lava lake crust and the mounds are interpreted to be geologically very recent lava extrusions (<100 Ma), in contrast to the surrounding very ancient mare shield deposits (∼3.5 Ga; from Head & Wilson 2017).

Table 1
Theories for the Origin and Age of Ina/IMPs

Ina/IMP Origin Theory	Formation Age	Mode of Emplacement	Reference
Sublimation	Not provided	Mounds: mare-like deposits; floor terrain: possible sublimates	Whitaker (1972)
Small lava intrusions associated with a mare dome	Among the youngest lunar volcanism, but specific age not provided	Entire Ina feature: small shield volcano summit caldera; mounds: small volcanic eruptions	El-Baz (1972, 1973); Strain & El-Baz (1980)
Gas release–induced surface regolith removal	Surface exposure age: <10 Ma; Crystallization age: >3.5 Ga	Exposure of buried ancient mare basalts by outgassing	Schultz et al. (2006)
Lava flow inflation	Not provided	Mounds: inflated lava flows; floor hummocky units: lava breakouts	Garry et al. (2012)
Small basaltic eruptions	<100 Ma	Mounds: small lava extrusions; floor units: lava pond crust	Braden (2013); Braden et al. (2014)
Pyroclastic eruption (proposed only for Cauchy 5 IMP, not for Ina)	Not provided	Pyroclastic deposits	Carter et al. (2013)
Lava lake processes and magmatic foam extrusion	∼3.5 Ga	Floor units: solidified lava lake crust; mounds: solidified magmatic foams	Qiao et al. (2017, 2018, 2019, 2020a, 2020b); Wilson & Head (2017b).

basaltic mare deposits, rather than being contained within a depression (Figure 4). One of the largest IMPs, Cauchy 5 in eastern Mare Tranquillitatis, offers a unique hybrid example of the two IMP types: a large pit crater–type IMP on the shield summit vent floor and hundreds of small mare-type IMPs on the shield flanks (Qiao et al. 2020b). This hybrid IMP provides an excellent opportunity to assess the genetic relationship between the two IMP subtypes. Qiao et al. (2017, 2018, 2019) analyzed two of the largest IMPs of the pit crater type, Ina and Sosigenes in western Mare Tranquillitatis, and proposed that the range of unusual geomorphologies and textures of the interior terrains of the largest lunar IMPs within pit craters can be explained as being due to lava lake activity involving highly vesicular/bubble-rich magma extrusion during the waning-stage evolution of a dike-tip pit crater, contemporaneously with the background mare basalts emplaced more than 3 Ga ago.

In this scenario, the hummocky and blocky floor terrains were described as a chilled lava lake crust, and the raised mounds were interpreted as final-stage extrusions of viscous magma with an extreme vesicularity, up to ∼95% (magmatic foams; Figure 4(a)). The unusual substrate characteristics of the final deposits, abundant macro- and microvesicularity for the floor terrains, and substantial microvesicularity for the raised mounds were interpreted to dramatically modify the nature of postemplacement surface modification processes, including impact cratering, regolith development and accumulation, erosion/disruption of topography, and space weathering, generating the range of highly unusual observed characteristics of Ina and leading to the anomalously young CSFD model ages reported by Braden et al. (2014). Using the hybrid geological relationships displayed at the Cauchy 5 IMP, Qiao et al. (2020b) concluded that the small mare-type IMPs were basically formed by a similar mechanism to that of the large pit crater–type IMPs but in different geologic settings (overflow on the rim and flank of the small mare shield volcano). In a nonshield volcano mare flow environment, the extruded highly vesicular magma foams, instead of being contained within a depression crater, would simply overflow beyond the vent rim and be emplaced on the adjacent exterior mare surface as thin foamy lava flows (lava flow Phase 4a of the eruption model of Wilson & Head 2018). Post-flow-emplacement impact events were interpreted to cause collapse in the void-rich flows, exposing the rough and coherent interiors of the foamy flows, as observed at many small mare-type IMPs (Figure 4(b)).

This scenario of waning-stage two-phase lava lake activity and magmatic foam extrusion is supported by a range of observations (Carter et al. 2013; Elder et al. 2017; Qiao et al. 2019, 2020b),

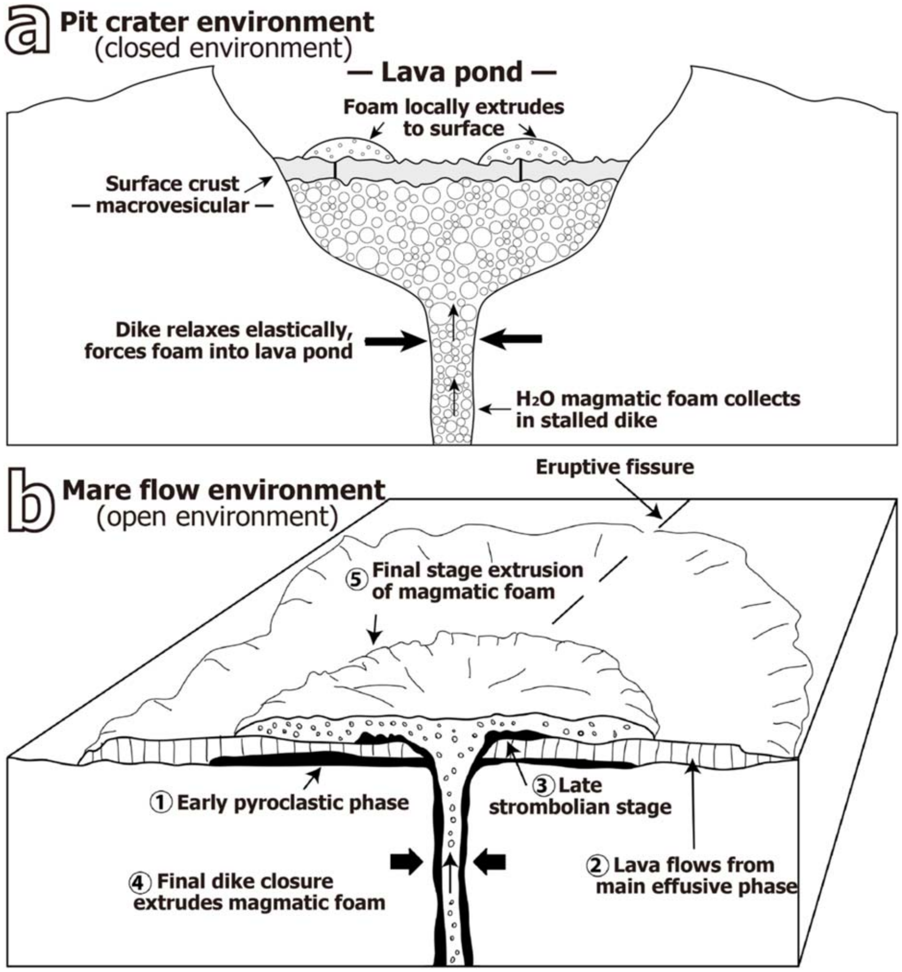

Figure 4. Models for late-stage foam-rich mare basalt extrusions in (a) pit craters and (b) unconfined fissure mare foam flow environments (from Wilson & Head 2017b). (a) Magmatic processes in the dike tip and summit vent during the final phases of a small lunar shield-building eruption (e.g., the shield underlying the Ina pit crater); shallow gas exsolution to produce very vesicular magmatic foams in the dike tip and vent floor lava lake, fracturing of the chilled and brittle lava lake crust, and squeeze-ups of the highly foamy lavas to form bulbous mounds. (b) Sequence of processes operating in a mare flow eruption from a fissure vent. Similar magmatic processes to the pit crater settings (a) are also illustrated here, but due to the lack of a confining dike-tip pit crater/vent, the highly vesicular foamy lava extrudes as a broader and thin lava flow. Postemplacement impacts into these solidified void-rich lava flows produce many of the small-scale IMPs observed in lunar maria (Braden et al. 2014; Qiao et al. 2020a).

including (1) the spatial density disparity of superposed impact craters between the interiors of IMPs (both floor and mound units) and the surrounding mare surfaces, (2) the unconsolidated substrate nature of the Ina mounds derived from Diviner thermophysical measurements, (3) the fine-grained and block-free nature of the small mare-type IMP materials from Arecibo radar mapping data (for Cauchy 5), and (4) the high reflectance and optical immaturity of the IMP deposits. The waning-stage magmatic foam eruption scenario is further supported by recent theoretical assessments of magma ascent and eruption in the final phases of activity in volcanic pit craters/vents (Wilson & Head 2017b) and lava flows (Head & Wilson 2017; Wilson & Head 2017a, 2018). These authors predicted that, during the late-stage activity of lava lakes and fissure eruptions, the magma ascent rate decreased greatly, and shallow gas exsolution in the dike produced highly vesicular magmatic foams. Final-stage dike stress relaxation and dike closure would slowly squeeze the foamy magma out of the dike, cracking the partly solidified lava lake floor and extruding the convex-upward mounds.

In summary, the hypotheses for the origin of Ina can be subdivided into two categories (Table 1).

(1) *Formation age.* (a) Geologically extremely young, as indicated by the CSFD ages of ∼33 Ma, optical immaturity, and sharp contacts; (b) geologically ancient, coincident with the ∼3.5 Ga age of the surrounding shield volcano, with other factors explained by unusual substrate characteristics; and (c) hybrid, geologically old but rejuvenated by recent activity (outgassing).

(2) *Setting and mode of emplacement.* (a) Formation in the summit pit crater of an ancient shield volcano, (b) formation in the summit pit crater of an ancient shield volcano but due to magmatic activity ∼3.4 billion yr later, (c) formation by flow inflation processes in a summit pit crater, (d) formation by late-stage volatile exsolution processes in the waning stages of an ancient shield volcano summit vent, and (e) formation by recent deep gas release processes in an ancient shield volcano summit pit crater.

2. Significance of the Age and Origin of Ina: The Thermal Evolution of the Moon

While Ina/IMPs are now generally considered to be volcanic in origin, the specific formation mechanism is still highly controversial (Table 1). One of the most contentious issues concerning Ina's origin is its emplacement age, especially between the geologically very recent (<0.1 Ga) small basaltic eruption model (Braden et al. 2014) and the ancient (>3 Ga) magmatic foam extrusion hypothesis (Qiao et al. 2017, 2018, 2019, 2020a, 2020b; Wilson & Head 2017b). On the basis of (1) the physical volcanological study of final-stage eruption processes and volatile exsolution patterns and (2) the detailed geological characterization of Ina's interior units, Qiao et al. (2017, 2018, 2019, 2020a, 2020b) and Wilson & Head (2017b) concluded that the interpreted magmatic foam substrate of the Ina mounds (abundant small vesicles with a bulk porosity up to ∼95%) would result in superposed impact events characterized by energy partitioning that favored crushing of the void space below the projectile trajectory at the expense of lateral ejection. Thus, crater diameters would be much smaller (∼20%–30% of the diameters of the same meteoritic impacts into typical mare regolith targets). Incorporating this "aerogel" effect of reduced impact crater diameter could readjust the observed crater retention age of less than 0.1 Ga to more than 3 Ga, coeval with the adjacent mare deposits. This ancient scenario complies with the conventional models of lunar geological and thermal evolutions, which predict that the continued net cooling of the Moon due to progressive heat loss by conduction caused mantle melting (magma source regions) to be deeper and much less abundant and the global state of stress in the lithosphere to be increasingly contractional with time (Solomon & Head 1980; Head & Wilson 1992, 2017; Shearer et al. 2006; Ziethe et al. 2009). These factors combined to gradually inhibit the generation, ascent, and eruption of basaltic magma on the Moon, causing mare volcanic activity to diminish in the middle of lunar history (Eratosthenian Period) and eventually cease in the last ∼1 Ga (Copernican Period; Hiesinger et al. 2011; Morota et al. 2011).

The geologically very recent small volcanic eruption origin scenario (Braden et al. 2014), however, raises a line of questions that conflicts with the above lunar evolution model and indeed requires the overall evolution history to be very different: (1) the current lunar interior would need to be much hotter than previously thought, thus being able to maintain considerable amounts of material near the melting point; (2) the abundance of heat-producing elements (mainly Th, U, and K) in the lunar interior would have to be much higher than prior estimations; and (3) at least parts of the lunar lithosphere might be currently extensional in a net state of stress, thus assisting magma in the deep lunar interior in its ascent to the surface to erupt. In addition, the IMPs are widely spread across the nearside maria, and half of them are outside the Procellarum KREEP Terrane, implying that significant heat sources in many portions of the lunar interior persist to geologically very recent time in order to account for the abundant small-volume IMP eruptions. A major reassessment of the current models of lunar thermal evolution would be required if the very young volcanic eruption origin for Ina/IMPs is verified.

3. Synthesis of Predictions of the Two End-member (Young and Old) Models

Current debate on the age and origin of Ina/IMPs centers on these two competing theories: (1) geologically very young (late Copernican) small-volume volcanic activity (Braden et al. 2014) and (2) ancient (Imbrian) volcanic eruption producing highly vesicular magmatic foams (Qiao et al. 2017, 2018, 2019, 2020a, 2020b; Wilson & Head 2017b).

3.1. The Young Model

In the late Copernican volcanism scenario (Figure 3), the uneven/hummocky floor terrains are solidified lava lake crust within the shield summit vent being disrupted by lava drainage and deflation, and the smooth mounds are subsequent small lobate lava flows extruded through the cracked floor crusts (Braden 2013; Braden et al. 2014). The mounds within Ina are 2–20 m thick (relative to the floor terrains), with an average value of 8 m, overlapping with the thickness range of mare basalt flows (e.g., Schaber 1973; Hiesinger et al. 2002). The convex-upward Ina mounds exhibit steep marginal scarps with an average margin slope of 26° (14°–39°, 6 m baseline), another piece of evidence supporting a very young age for the Ina deposits.

Among the questions raised about the young volcanism interpretation are the following.

(1) Continued net cooling of the Moon since the middle of lunar history would have decreased the average mantle temperature gradually, causing mantle melting to be less abundant and magma source regions to be deeper. On the basis of terrestrial analog observations (Hardee 1980), theory, and conductive cooling calculations (e.g., Wilson & Head 1981, 2017a), the lava pond in the Ina IMP could not have remained molten, following the last eruption, for more than a few hundred to a thousand years and thus is not a source for eruptions occurring more than 3 billion yr later. Bruce & Huppert (1989), Gonnermann & Taisne (2015), and Wilson & Head (2017a, 1981, 1988) also show that any magma in the dike connecting the source region to the surface would cool and solidify even more rapidly. It is also highly unlikely that the magma source region for the Ina shield volcano (at several hundred kilometers in depth) could remain molten for the 3.4 Ga long interval between the Ina shield-building eruption and any geologically very recent small magma extrusions within the 2 × 3 km summit vent; such individual source regions are typically not active for times in excess of tens to hundreds of millions of years (e.g., Shearer et al. 2006; Wieczorek et al. 2006; Marsh 2015; Wilson & Head 2017a).

In addition, in order to extrude magma onto the surface from a molten source region located at the great depth thought to be typical of the last several hundred million years (Shearer et al. 2006; Wieczorek et al. 2006), a higher excess pressure of basaltic diapirs (hence, greater magma source volume) is required to reach the surface from such a deeper magma source region. It seems highly implausible that magma would erupt from such a great depth and then be erupted in such small amounts (e.g., Head & Wilson 2017; Wilson & Head 2017a).

(2) The shield volcano underlying the Ina summit pit crater is apparently very ancient (e.g., Garry et al. 2012), dated to be ∼3.5 Ga through crater population analysis (Qiao et al. 2017, 2019), and thus formed during the major global lunar mare volcanism phase ∼3.3–3.8 Ga ago (Hiesinger et al. 2011). Conventional models of lunar thermal evolution predict that, after ∼3.5–3.6 Ga ago, cooling of the outer portion of the Moon produced increasingly compressive stress in the lunar lithosphere (Solomon & Head 1980). Could magma rise from significant depths in the recent thermal history of the Moon (in the last several hundred million years) along preexisting fractures (induced by large impacts or rising diapirs)? Given the increasing overburden pressure with depth and the thicker recent lithosphere (e.g., Wieczorek et al. 2006), the closure of faults and cracks occurs at relatively shallow depths

(Head & Wilson 2020b), and it is thus highly unlikely that preexisting fractures would have remained open as pathways for rising magma for over 3 Ga. For these reasons, the required dike propagation to the surface for volcanic eruptions would be progressively more difficult with time in the period following the initial Ina shield-building eruption. These factors suggest that it is improbable that volcanic activity at the small Ina site would recur very recently after having being dormant for ∼3.4 Ga, with no evidence of at least discontinuous activity during this long period.

(3) Imaging spectroscopic analysis shows that both the raised mounds and floor units within Ina have a high-Ca pyroxene-dominated mineral composition similar to that of the adjacent mare deposits (Bennett et al. 2015). This is surprising, in that the young volcanism model thus predicts that the magma reservoir or source region underwent no fractional crystallization or contamination by fresh magmas in the ∼3.4 Ga interval. Although Bennett et al. (2015) stated that "a possible solution is that both the mare and Ina were sourced from the deep mantle, which likely would not change its composition greatly, even over such a long period of time," it seems much more likely, on the basis of the mineralogical diversity of mare basalts in individual locations with geologic time (e.g., Hiesinger et al. 2011), that the composition would not remain the same. Thus, it seems more plausible that the multiple geological units within Ina were emplaced contemporaneously with the background mare deposits ∼3.5 Ga ago.

(4) The raised smooth mounds of Ina are among the most unusual terrains on the lunar surface, with a range of morphological peculiarities, including convex-upward bulbous shapes and marginal scarps and moats. Some young Eratosthenian lava flows in southwestern Imbrium are also observed to exhibit marginal scarps, but topographical moats are not observed at their flow margins (Schaber 1973). If these Ina mounds are normal lava flows, why is their morphology so different from that of other mare basalts? For example, the meniscus-like morphology (irregular, bleb-like shape with steep marginal slopes) is unlike any morphology identified on the Moon in typical basaltic landforms and deposits emplaced with basaltic lava rheology (Head & Wilson 2017).

(5) Diviner thermophysical mapping results for Ina indicate that the Ina interior is mantled by a surface regolith layer of measurable thickness (>10–15 cm; Elder et al. 2017). Synthesizing other thermophysical measurements, including thermal inertia, Elder et al. (2017) proposed some process such as explosive outgassing or pyroclastic eruptions as the origin of Ina and other lunar IMPs. Accumulation of a regolith layer of such thickness on geologically very young lava flows (∼33 Ma) seems unlikely and would require an unusually rapid development rate of lunar surface regolith (estimated to be 0.85 mm Ma^{-1} over the last billion years by Quaide & Oberbeck 1975, a 33 Ma old lava flow would accumulate a layer of regolith materials only ∼2.8 cm thick).

(6) Basilevsky & Michael (2020, 2021) showed that the morphology of young craters superposed on the Ina mounds is identical to that of craters on typical ancient mare surfaces and interpreted this to disprove the hypothesis that the mounds are formed of magmatic foams, and that this supports the relatively recent origin of the mounds. However, it has been documented (Zanetti et al. 2017; Plescia & Robinson 2019) that craters superposed on tens of millions of years old impact melt deposits (fresh solidified bedrock) in large young craters have very different morphology from those in mature regolith. Thus, if the mounds were indeed young effusive basaltic volcanic features, we would expect small crater morphologies to be similar to those in young impact melts. Thus, the arguments of Basilevsky & Michael (2020, 2021) could be cited to support an ancient age for the mound material.

3.2. The Old Model

The Imbrian-age volcanic eruption model provides an alternative interpretation for the age and origin of Ina and IMPs. In this scenario, the formation of various morphological units within Ina is basically the natural consequence of the latest stage of dike emplacement and magma degassing in the summit crater atop a small lunar shield volcano ∼3.5 Ga ago (Figure 4). Specifically, the floor hummocky units are interpreted as a chilled lava pond crust and the raised mounds as final-phase small magma extrusions (Qiao et al. 2017, 2018, 2019, 2020a, 2020b; Wilson & Head 2017b). In addition, waning-stage summit pit/vent activities under the unique lunar conditions of low gravitational acceleration and essentially zero atmospheric pressure produce unusually vesicular eruption deposits neither predicted nor observed on terrestrial final-stage eruptions. Extremely porous macrovesicular lava lake floor deposits are interpreted to favor drainage of subsequently produced regolith into the substrate and enhance the retention of optical immaturity and blockiness. Mounds are interpreted as the viscous extrusions of foamy magma that had collected below the lava lake floor in the terminal stages of the eruption. The highly vesicular substrate property of the extruded mounds is interpreted to exert notable effects on the postemplacement impact cratering process (energy partitioning) and produced anomalously young crater retention ages (<0.1 Ga).

Difficulties and critical unresolved issues also characterize the ancient, shield-contemporaneous summit lava lake magmatic foam eruption interpretation for Ina.

(1) How to convincingly explain the deficit of superposed impact craters and the resulting extremely young CSFD model ages of Ina interior deposits? Although the predicted unusually porous substrate characteristics of the Ina mounds and the consequent crater size decrease effect have been called on to account for the young crater counting ages of the Ina interior (Qiao et al. 2017, 2019; Wilson & Head 2017b), it should be noted that the consequences of impact cratering into highly porous materials and its effect on crater sizes are not yet fully understood due to many difficulties in both laboratory impact experiments and numerical simulations. Additional dedicated theoretical, experimental, and numerical studies of impact cratering into porous substrates should help to clarify the age debate on Ina and lunar IMPs and would also enhance our knowledge of surface processes on many porous asteroid bodies.

(2) Meteoritic impacts into the Ina foamy mounds were predicted to produce smaller, deeper ("cylinder-like" or "hole-like"), and nonblocky craters (Qiao et al. 2017; Wilson & Head 2017b). However, no such unusual craters are apparently seen on the Ina mounds (Basilevsky & Michael 2020, 2021). Instead, many impact craters superposed on the smooth mounds exhibit a range of characteristics of typical impact craters developed on mare regolith, including raised rims, ejecta deposits, blocky interiors, a range of degradations, and smaller depth-to-diameter ratios (Wagner et al. 2018; Basilevsky & Michael 2020, 2021). This appears to contradict the foam origin model for the Ina mounds. Additional

work on the nature of "autoregolith" development on extruded foamy lavas (e.g., Wilson & Head 2017b) needs to be undertaken, as does work on the nature of basaltic volcanic protoliths in general (e.g., Head & Wilson 2020a).

(3) The Ina floor terrains, especially the floor rubble materials, are characterized by unusually high reflectance and optical immaturity (Schultz et al. 2006; Garry et al. 2013; Bennett et al. 2015; Qiao et al. 2019). Any materials exposed to the harsh space environment of the lunar surface, including micrometeorite bombardment, cosmic- and solar-ray irradiation, and solar wind implantation, are equally subject to space weathering modification processes (Pieters & Noble 2016). Over a >3 Ga period of space weathering processes, significant modification of the optical properties of the Ina floor materials should occur, resulting in surface darkening and optical maturation, possibly resembling that of the mare regolith surface surrounding the Ina pit crater. Although the conceptual model of regolith drainage into the predicted macrovesicular void space of the lava lake floor may be plausible, a quantitative model to account for this process, the filling of the void space, the drainage-inducing processes, and the associated effects on optical maturation have not yet been formulated. Thus, it is unknown whether the model-predicted porous substrates have significant effects on space weathering processes on the lunar surface and, if so, how these effects map out into specific observed optical alteration properties.

(4) The contacts between Ina mounds and floor terrains are typically characterized by very steep scarps and adjacent moats, some of which have the steepest topographic slopes (=32°) on the Moon (Qiao et al. 2019), leading Fassett & Thomson (2015) to propose that these troughs must have been formed within the last 1–2 Ma or perhaps are still currently forming. Any ancient model of Ina origin must also explain how to maintain the very sharp contacts at Ina over 3.5 billion yr in a progressive topographic erosion environment predominantly induced by a steady impact crater flux, which serves to topographically smooth and mute such distinctive surface relief over time (Fassett & Thomson 2014). Although the moats have been attributed to subsurface foam evacuation, loading, flexure, and regolith drainage (e.g., Wilson & Head 2017b), it is still intuitively unclear how these processes could result in such sharp and distinctive moats and contacts.

3.3. Summary

We thus conclude that in order to resolve the differences between these two hypotheses for the origin of Ina, new data, experiments, and missions are required. In the following sections, we first identify the key observations and measurements that would help distinguish between the two models, and then we define a range of mission types that could be undertaken to provide these data. For simplicity, we refer to the Braden et al. (2014) hypothesis (Figure 3) as the Ina-is-younger model (young model) and the Qiao et al. (2017, 2019) shield-contemporaneous ∼3.5 Ga model as the Ina-is-older model (old model).

4. Key Observations and Measurements to Distinguish between the End-member Models

In this section, we list a sequence of key observations and measurements from the Ina surface and samples that would help explain the range of enigmatic features in Ina and resolve key questions concerning its origin, especially the "age question": what is the age of the units comprising the Ina IMP (mounds and floor unit)? Is it concurrent with the emplacement of the small shield volcano and surrounding mare deposits and thus over 3 billion yr old? Was it formed in the last few tens of millions of years, as interpreted from superposed impact CSFDs? We also assess the "mode of origin of the units question": what is the origin of the units comprising the Ina IMP (mounds and floor unit)? Are they due to the minor variations in the typical lunar mare basalt lava flow emplacement processes? Or are they due to the major variations in the vesicularity and physical properties of basaltic magmas intruded in the terminal phases of shield volcano summit pit crater eruptions? In particular, these observations and measurements would help distinguish between the two end-member models: the young model (Braden et al. 2014) and the old model (Qiao et al. 2017, 2019).

(1) *Radiometric ages of the Ina mounds and floor materials.* Acquisition and radiometric dating of samples of the material that makes up the mounds and floor units would provide unequivocal evidence to distinguish between the two models. These measurements are necessary and sufficient to unambiguously resolve the key question concerning the formation age of Ina deposits. The magnitude of the age difference between the two models (>3.4 Ga or a factor of over 100) is so large that perhaps even in situ age determination (e.g., Anderson et al. 2017) could resolve the controversy.

(2) *Characteristics of the regolith material on the mounds and floor.* Predictions of the young model suggest that the regolith is derived from recently emplaced basalts and thus the regolith development from this protolith (Head & Wilson 2020a) should be standard impact fragmentation of solid basalt to produce a regolith. The old model, on the other hand, predicts that the mound protolith will be very vesicular magmatic foam, with an "autoregolith" of explosively fragmented bubble wall shards and an impact-induced regolith produced from and on top of this substrate. The floor unit is predicted to be composed of macrovesicular basalt with regolith draining into the void spaces, leaving larger and optically immature particles and rocks on the surface. Thus, there should be a clear distinction possible between the two models on the basis of the predicted substrate characteristics. In situ observations (high-resolution images of regolith particles in both terrains to assess their grain size, shape, optical maturity, agglutinates, proportion of glass, etc.), sieves to assess particle size distributions, and observations to assess the nature of the moats and search for evidence of macrovesicular voids and associated regolith drainage in the floor units and subunits, would easily distinguish the two origin models. In addition, detailed Ina regolith property analyses would also help test or verify other formation theories of Ina (Table 1). For instance, if typical normal mare regolith characteristics are observed, they are also consistent with the recent gas release–induced removal of the ancient regolith model (Schultz et al. 2006).

(3) *3D structure of the mounds and floor material (porosity).* Emplacing core tubes in the upper meters of the floor and mound regolith deposits would be a significant step in documenting the vertical structure, variability, and origin of the regolith. A much more comprehensive view could be obtained by ground-penetrating radar (GPR) surveying (e.g., Xiao et al. 2015; Lai et al. 2019; Li et al. 2020) of the mound and floor units. Seismic profiling could also determine the nature of the mound and floor unit 3D structure and readily

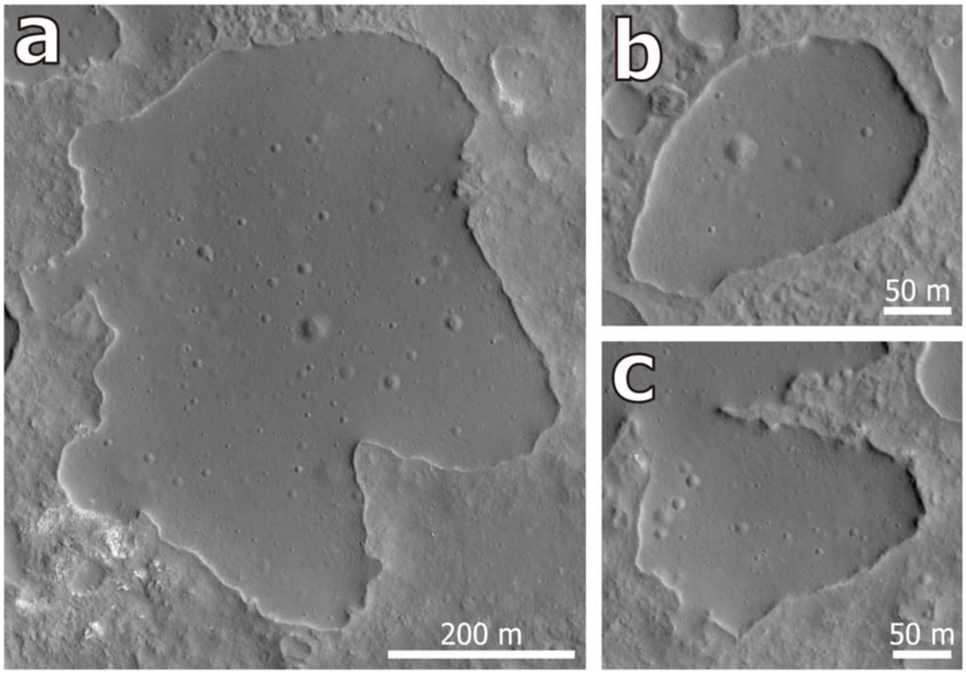

Figure 5. The LROC NAC images of mound terrains (all cropped from frame M119815703) proposed as landing targets for robotic lander and/or sample return missions.

distinguish between the normal basaltic substrate of the young model and the highly macro- and microvesicular nature of the old model.

(4) *Regolith thickness; any change with depth on mound and floor material*. Comparison of regolith thickness (and nature) through coring, GPR, and seismic studies will also be critical in distinguishing between the old (thicker and more mature regolith developed over >3.4 Ga) and young (much thinner and patchy regolith developed over ∼33 Ma) models.

(5) *Nature of ejecta from craters into mound and floor material*. Assessment of the morphology and frequency distribution of superposed impact craters of different sizes will help in identifying any distribution that might deviate from standard basaltic morphologies and proportions or, alternatively, that might signal the presence of a substrate or regolith of a foamy or macrovesicular nature. Analysis and sampling of crater ejecta from different-sized craters will also reveal changes in the substrate with depth that will distinguish between the old and young model predictions.

(6) *Level of vesicularity of surface rocks*. Surface observation and analysis of crater ejecta indicating subsurface layers and their level of vesicularity will also help to distinguish between the two hypotheses, with old model predictions requiring very significant macrovesicularity in the floor units and magmatic foam-level vesicularity in the mound unit.

(7) *Volatile content of magma petrogenesis*. Return of samples to Earth for laboratory analysis and petrogenetic probing will provide essential data to identify the depth of origin of magmas, petrogenetic pathways, and the nature and amount of volatiles necessary to produce magmatic foams.

(8) *Comparison of rocks, soils, and ages inside Ina and on the shield rim*. An extended traverse to the Ina shield volcano rim and flanks, the collection of samples there to compare with those collected on the floor of Ina, and analysis of comparative ages, vesicularities, and petrogenesis would provide conclusive evidence to distinguish between the old and young models for the origin of Ina.

(9) *Paleomagnetism measurements*. In situ magnetic analyses, or laboratory analysis of returned samples, would provide important evidence to distinguish between the two hypotheses. Magnetized samples would support the old hypothesis, as the lunar magnetic field is interpreted to have been active at ∼3.5 Ga but decayed by the time (∼33 Ma) derived from CSFD ages (Weiss & Tikoo 2014).

5. Missions Capable of Addressing These Objectives

In this section, we present an assessment of several mission styles and modes, optimal landing sites, and, where appropriate, conceptual traverses. We conclude with a human landing and exploration design reference mission (DRM).

(1) *Robotic lander mission (with or without hopping mobility)*. A single robotic lander mission with no mobility (e.g., Stopar et al. 2019) could significantly contribute to distinguishing between the two hypotheses by carrying a payload consisting of a high-resolution multispectral imager, a microscopic imager for grain size and morphology, a magnetometer, a scoop to dig into the subsurface and assess the mechanical properties of the regolith, an in situ GPR as manifested on the Chang'e-5 lunar lander (Li et al. 2019b; Xiao et al. 2019), and, if possible, an in situ geochronology instrument to clarify the age debate of Ina deposits (e.g., a K-Ar laser experiment developed by Cohen et al. 2014). If limited to a single mission, the spacecraft should land on a mound on the floor of Ina (e.g., Stopar et al. 2019 and Figure 5), as the mound characteristics (basaltic regolith versus magmatic foam regolith and autoregolith) are the most prominent predictions to distinguish between the two models and test other formation theories of Ina (Table 1).

Hopping capability would significantly assist in assuring representative measurements and determining diversity within the mound, and long or multiple hops might permit access to

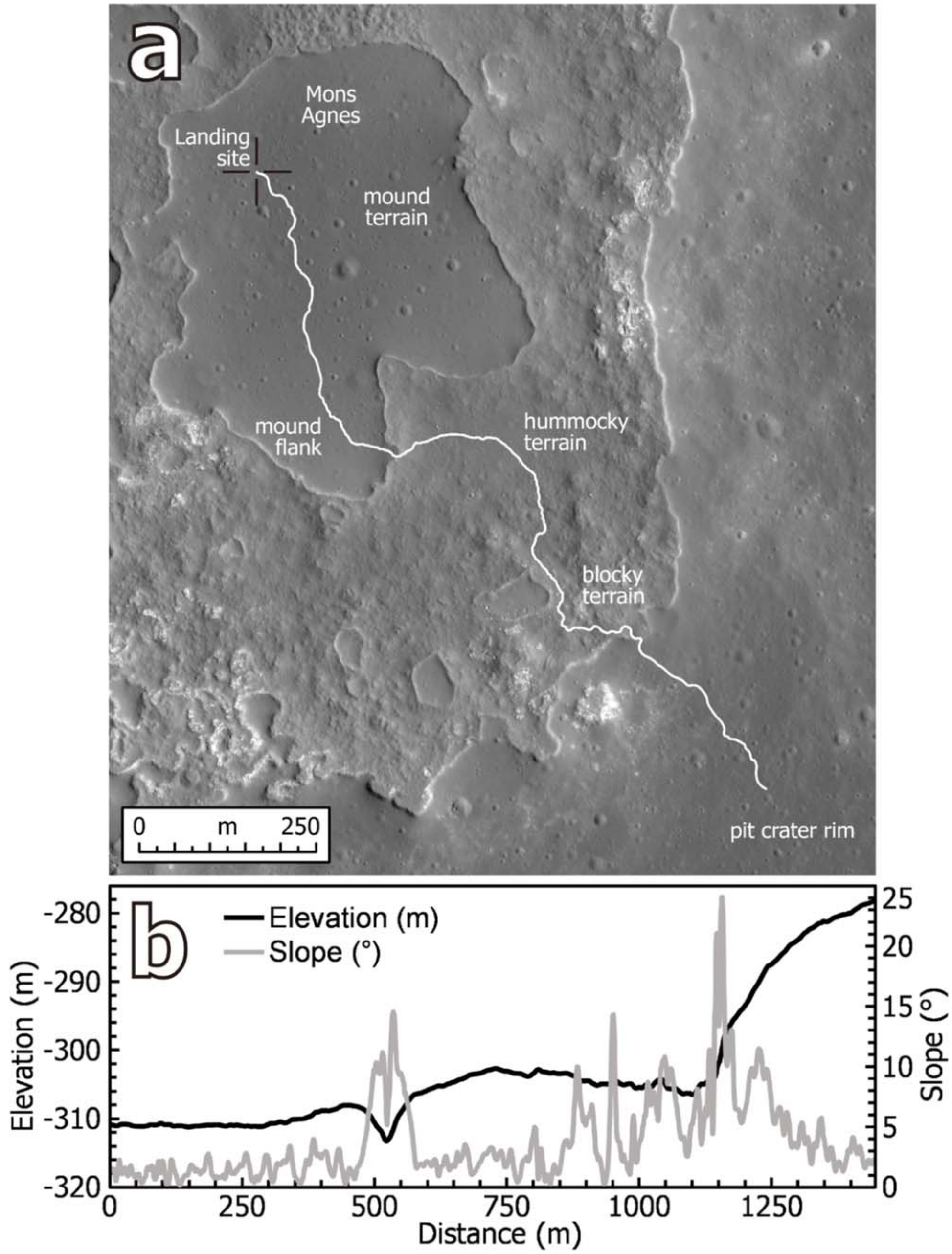

Figure 6. (a) Proposed landing site (marked by the black crosshair) and traverse path for a robotic rover mission to the Ina pit crater; surface investigation sites are labeled. The background is cropped from LROC NAC frame M119815703. (b) LROC NAC DTM elevation (black line) and slope (gray line) profiles along the traverse path.

the floor units as well. Multiple landing missions would also accomplish these goals.

(2) *Robotic sample return mission*. The most conclusive results to distinguish between the models would result from a sample return mission. A robotic probe, similar to the Chang'e-5 sample return mission profile (Li et al. 2019a), to a mound landing site would be ideal (e.g., Figure 5), with imaging systems to document the local setting, GPR to probe the subsurface regolith and bedrock structure, a scoop to assess the upper parts of the regolith and collect samples, and a meter-scale core to sample with depth. Returned to Earth, these samples could be fully assessed from a geologic, chronologic, geophysical, and petrogenetic perspective, and a clear and concise answer could be obtained.

(3) *Robotic rover mission.* The addition of mobility to a lander mission would significantly enhance the science return and not only distinguish among the hypotheses but also help to understand the actual array of processes involved in the formation of the Ina structure (and similar features such as Sosigenes, Cauchy 5, and the population of smaller IMPs; Braden et al. 2014; Qiao et al. 2020a). For example, rovers could traverse from a landing on the relatively smoother mounds to the mound flanks, the various units on the Ina floor, and perhaps even the rim of the pit crater to compare and contrast the characteristics of the Ina floor with those of the shield volcano itself (Figure 6). Traverse geology (imaging and trafficability), geophysics (magnetic, seismic, and GPR traverses), detailed sample analyses (multispectral mineralogy and microscopic imaging), as well as the ability to probe the upper meters of regolith (scoops and rover tracks), are also essential.

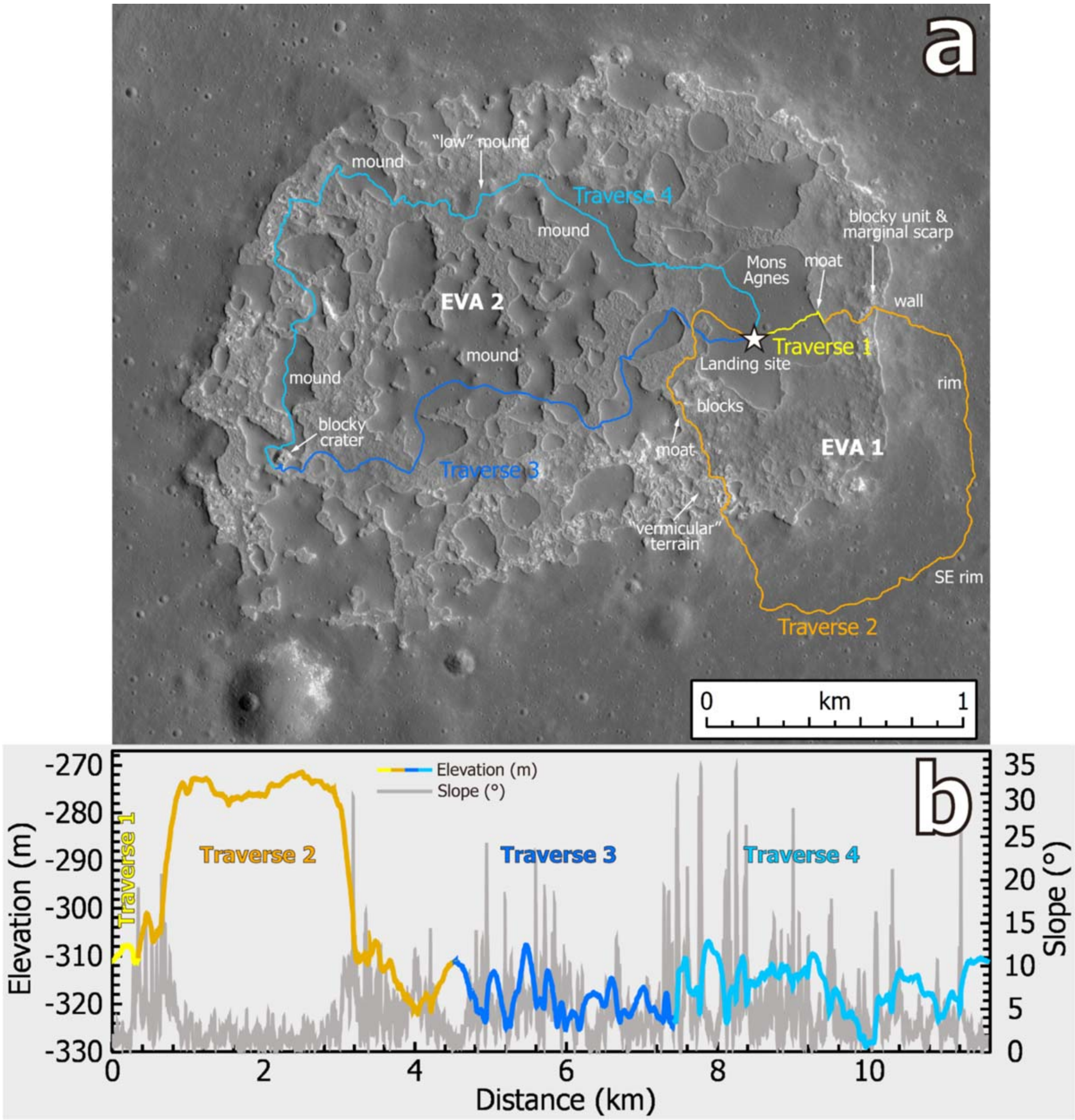

Figure 7. (a) Traverse map of our proposed human landing and exploration DRM to the Ina pit crater and vicinity, showing the suggested landing site (star) on the largest mound (Mons Agnes), astronaut traverse paths during the first (including traverses 1 and 2) and second (including traverses 3 and 4) EVA, and scientific investigation sites (labeled by terrain names). The background is cropped from LROC NAC frame M119815703. (b) LROC NAC DTM elevation (colored line) and slope (gray line) profiles along the traverse paths.

(4) *Human landing and exploration mission.* With a resurgence of interest in lunar exploration, including China's continued Lunar Exploration Program, the NASA program "Forward to the Moon with Artemis," and the parallel and cooperative human exploration endeavors of the ESA, Russia, India, and others, human exploration of the Moon is clearly feasible in the first half of the 21st century. Here we present a DRM for an Apollo J-Mission-scale expedition to the Ina summit pit crater and vicinity (Figure 7), designed specifically to resolve the issue of the two (old and young) origins for the Ina crater interior but, more importantly, to provide the data to establish a refined or new model that can help explain these enigmatic features in Ina, as well as other large features, such as Sosigenes and Cauchy 5, and the many dozens of smaller IMPs in the lunar maria (e.g., Braden et al. 2014; Qiao et al. 2020a).

In this DRM (Figure 7), we propose landing on the floor of Ina on the largest of the mounds (formally named Mons Agnes; Figure 7), deploying Apollo Lunar Surface Experiments Package–like geophysical monitoring stations, and undertaking extensive coring and analysis of the regolith and substrate of the mounds, sampling laterally within walking distance with meter-scale cores and extensive geologic observations and sampling guided by astronaut visual observations and in situ GPR data. Following the first extravehicular activity (EVA; yellow path in Figure 7), the crew would traverse due east, down the flanks of the mound, across the moat (labeled in Figure 7), stopping to examine the characteristics and morphology of the moat structure, before proceeding across the more mature floor regolith deposits. Samples and observations here from traverse geophysics and GPR data will help measure the substrate density and search for evidence of macrovesicularity predicted by the old model. The second traverse (gold path in Figure 7) continues to the bright and optically immature blocky unit and outcrops at the eastern margin of the Ina floor (labeled in Figure 7), where stratigraphy may also be exposed in the marginal scarp. Following analysis of the floor margin contact, the traverse would continue up the wall of the pit crater to the rim to continue geophysics and sampling to compare the ancient rim of the shield volcano with the potentially >3 Ga younger floor (Figure 7). The traverse would then extend along the southeast rim of the pit crater, obtaining perspective views and measurements of the Ina interior, and then descend down to the pit crater floor at the "vermicular" terrain before heading to the western margin of the largest Ina mound and moat and ascending the mound back to the landing site (Figure 7). The total traverse distance of the first EVA would be about 3.2 km, a modest distance compared with Apollo J-Mission traverses. The second EVA (traverse 3, shown as the blue path in Figure 7) would traverse from the landing site in a west–southwest direction, crossing multiple mounds for comparison with the major mound, its moat margins, and the intervening floor subunits, and would have as a target an unusual blocky impact crater on the southwest Ina floor (Ivanov & Head 2019; labeled in Figure 7). Here, exploration and analysis of the unusual nature of impact craters and the stratigraphic relationships between mounds and floor units will significantly assist in the determination of the origin of the Ina floor deposits and the specific processes operating to form them. A fourth traverse (cyan path in Figure 7) explores the northern and northwestern part of the Ina floor, providing additional characterization of the Ina floor units and their 3D structure. The astronauts would traverse down onto a peculiar "low" mound feature (labeled in Figure 7) in the northern floor. This low mound is $\sim 100 \times 80$ m in size, the largest one among six low mounds identified in the Ina interior floor with smooth surface textures and lower elevations than the surrounding terrain (Qiao et al. 2019). These extensive geologic field investigation and sampling of Ina's materials will provide fundamental insights into its characteristics and formation mechanisms. Together, these four traverses cover a total distance of about 11.6 km (Figure 7), well within the range for the successful Apollo J-Missions (∼28–36 km in Apollo 15, 16, and 17). Clearly, human exploration and the associated mobility provide significantly more scientific results than can be obtained by a robotic mission alone.

However, the nature of the slopes and the physical structure of the regolith along the proposed traverses (Figures 6 and 7) may present some challenges to human and robotic exploration. For example, the slopes at the margins of the mounds in our traverse may sometimes exceed those encountered by the Lunokhod and Apollo rovers (Basilevsky et al. 2019); thus, engineering designs and operational strategies need to take this into consideration. In addition, the macroporosity and regolith characteristics predicted by some models (e.g., magmatic foam mounds and macroporous floors; Qiao et al. 2017, 2019; Wilson & Head 2017b) may introduce potential trafficability and soil particle contamination problems that should be taken into consideration during mission planning (e.g., including GPR instruments and designing the rovers to accommodate very fine angular particles).

6. Conclusions

The Ina pit crater is one of the most mysterious lunar features identified and investigated during the Apollo era (Whitaker 1972; El-Baz 1973). Its range of geological peculiarities has perplexed lunar scientists for decades and resulted in a wide variety of hypotheses for their origins. Ina is also the most notable representative of a group of dozens of small mare features identified on high-resolution LROC NAC images and termed IMPs (Stooke 2012; Braden et al. 2014). However, the specific formation mechanism and emplacement age of Ina and other lunar IMPs have been long debated, and various competing theories have been proposed to account for the characteristics, age, and origin of Ina/IMPs (Table 1). One of the most contentious issues concerning Ina's origin is the actual emplacement age, especially the disparity between the geologically very young (<0.1 Ga) small volcanic eruption model (young model; Braden et al. 2014) and the very old (>3 Ga) magmatic foam extrusion hypothesis (old model; Qiao et al. 2017, 2018, 2019, 2020a, 2020b; Wilson & Head 2017b). Distinguishing between the two competing theories will provide vital constraints on the cessation time of lunar mare volcanism, either the previously established ∼1 Ga ago (Hiesinger et al. 2011; Morota et al. 2011) or the recently proposed geologically very recent ∼18 Ma (Braden et al. 2014); this is a key parameter for modeling the geological and thermal evolution of the Moon.

We conclude that in order to resolve the controversy between these two very different scenarios for the origin and age of Ina, new data, experiments, and sample returns from new landed lunar missions are required. To unequivocally resolve the question of the ancient or recent age of the Ina IMP, a robotic sample return mission, such as the recent Chang'e-5 mission (Li et al. 2019a), is required. In order to unequivocally resolve the question of the origin of the geologic units comprising the Ina IMP, a robotic rover or human exploration mission that can traverse and examine the soils, rocks, and substructure of the units is required. In this contribution, we identify key measurements from the Ina surface and on samples that would help distinguish between the two end-member models, including radiometric ages of Ina deposits, the nature of regolith materials, 3D shallow subsurface structure, volatiles involved in magma petrogenesis, and paleomagnetism. In the current international circumstances of a resurgence of lunar exploration endeavors, we define a range of conceptual lunar missions to the Ina feature, including mission styles, optimal landing sites, and conceptual traverses for robotic lander and/or rover missions, robotic sample return missions, and human landings and exploration. These missions will provide vital data not only to resolve the issue of the two (old and young) origins for the Ina crater interior but also, more importantly, to establish a refined or new model that can help explain these enigmatic features in Ina, as well as other large features, such as Sosigenes and Cauchy 5, and the many dozens of smaller IMPs in the lunar maria (e.g., Braden et al. 2014; Qiao et al. 2020a).

This study is supported in part by the National Key R&D Program of China (No. 2020YFE0202100), Pre-research Projects on Civil Aerospace Technologies Nos. D020205 and D020102 funded by CNSA, and the National Natural Science Foundation of China (Nos. 41703063, 11941001, and 41972322). J.W.H. gratefully acknowledges financial support from the NASA Lunar Reconnaissance Orbiter Lunar Orbiter Laser Altimeter (LOLA) experiment (grants NNX09AM54G and NNX11AK29G) at Brown University.

ORCID iDs

Le Qiao https://orcid.org/0000-0002-6180-2344
Lionel Wilson https://orcid.org/0000-0003-3284-3515

References

Anderson, F. S., Whitaker, T. J., Wiesendanger, R., et al. 2017, in 5th European Lunar Symp. 25 (Münster: Univ. Münster), 25
Basilevsky, A. T., & Michael, G. G. 2020, in 11th Moscow Solar System Symp. (Moscow: Space Research Institute), 209
Basilevsky, A. T., & Michael, G. G. 2021, SoSyR, 55, 20
Basilevsky, A. T., Krasilnikov, S. S., Ivanov, M. A., et al. 2019, SoSyR, 53, 383
Bennett, K. A., Horgan, B. H. N., Bell, J. F., III, Meyer, H. M., & Robinson, M. S. 2015, LPSC, 46, 2646
Braden, S. E. 2013, Analysis of Spacecraft Data for the Study of Diverse Lunar Volcanism and Regolith Maturation Rates (Tempe, AZ: Arizona State Univ.)
Braden, S. E., Stopar, J. D., Robinson, M. S., et al. 2014, NatGe, 7, 787
Bruce, P. M., & Huppert, H. E. 1989, Natur, 342, 665
Carter, L. M., Hawke, B. R., Garry, W. B., et al. 2013, LPSC, 44, 2146
Cernan, E. A., Evans, R. E., & Schmitt, H. 1972, Apollo 17 Technical Air-to-ground Voice Transcription (Houston, TX: Manned Spacecraft Center)
Cohen, B. A., Miller, J. S., Li, Z.-H., Swindle, T. D., & French, R. A. 2014, Geostandards and Geoanalytical Research, 38, 421
Defense Mapping Agency 1974, National Aeronautics and Space Administration Lunar Topophotomap (Washington, DC: Defense Mapping Agency Topographic Center), 41C3S1, (10)
El-Baz, F. 1972, LPSC, 3, 39
El-Baz, F. 1973, Apollo 17 Preliminary Science Report (Washington, DC: USGO), 30
Elder, C. M., Hayne, P. O., Bandfield, J. L., et al. 2017, Icar, 290, 224
Evans, R. E., & El-Baz, F. 1973, Apollo 17 Preliminary Science Report (Washington, DC: USGO), 28
Fassett, C. I., & Thomson, B. J. 2014, JGRE, 119, 2255
Fassett, C. I., & Thomson, B. J. 2015, LPSC, 46, 1120
Garry, W. B., Hawke, B. R., Crites, S., Giguere, T., & Lucey, P. G. 2013, LPSC, 44, 3058
Garry, W., Robinson, M. S., Zimbelman, J. R., et al. 2012, JGRE, 117, E00H31
Gonnermann, H., & Taisne, B. 2015, in The Encyclopedia of Volcanoes, ed. H. Sigurdsson (2nd ed.; Amsterdam: Academic Press), 215
Hardee, H. C. 1980, JVGR, 7, 211
Head, J. W., & Wilson, L. 1992, GeCoA, 56, 2155
Head, J. W., & Wilson, L. 2017, Icar, 283, 176
Head, J. W., & Wilson, L. 2020a, GeoRL, 47, e88334
Head, J. W., & Wilson, L. 2020b, P&SS, 180, 104765
Hiesinger, H., Head, J. W., Wolf, U., Jaumann, R., & Neukum, G. 2011, GSASP, 477, 1
Hiesinger, H., Head, J., III, Wolf, U., Jaumann, R., & Neukum, G. 2002, GeoRL, 29, 1248
Ivanov, B. A., & Head, J. W. 2019, LPSC, 50, 1243
Lai, J., Xu, Y., Zhang, X., et al. 2019, GeoRL, 46, 12783
Li, C., Wang, C., Wei, Y., & Lin, Y. 2019a, Sci, 365, 238
Li, C., Su, Y., Pettinelli, E., et al. 2020, SciA, 6, eaay6898
Li, Y., Lu, W., Fang, G., Zhou, B., & Shen, S. 2019b, AdSpR, 63, 2267
Marsh, B. D. 2015, in The Encyclopedia of Volcanoes, ed. H. Sigurdsson (2nd ed.; Amsterdam: Academic Press), 185
Morota, T., Haruyama, J., Ohtake, M., et al. 2011, E&PSL, 302, 255
Pieters, C. M., & Noble, S. K. 2016, JGRE, 121, 1865
Plescia, J. B., & Robinson, M. S. 2019, Icar, 321, 974
Qiao, L., Head, J., Wilson, L., et al. 2017, Geo, 45, 455
Qiao, L., Head, J. W., Ling, Z., et al. 2019, JGRE, 124, 1100
Qiao, L., Head, J. W., Ling, Z., & Wilson, L. 2020a, JGRE, 125, e06362
Qiao, L., Head, J. W., Wilson, L., & Ling, Z. 2020b, JGRE, 125, e06171
Qiao, L., Head, J. W., Xiao, L., Wilson, L., & Dufek, J. D. 2018, M&PS, 53, 778
Quaide, W., & Oberbeck, V. 1975, Moon, 13, 27
Robinson, M. S., Brylow, S. M., Tschimmel, M., et al. 2010, SSRv, 150, 81
Schaber, G. G. 1973, LPSC, 4, 73
Schultz, P. H., Staid, M. I., & Pieters, C. M. 2006, Natur, 444, 184
Shearer, C. K., Hess, P. C., Wieczorek, M. A., et al. 2006, RvMG, 60, 365
Solomon, S. C., & Head, J. W. 1980, RvGeo, 18, 107
Stooke, P. J. 2012, LPSC, 43, 1011
Stopar, J. D., Lawrence, S. J., Samuel, J., et al. 2019, P&SS, 171, 1
Strain, P. L., & El-Baz, F. 1980, LPSC, 11, 2437
Wagner, R., Denevi, B. W., Stopar, J. D., van der Bogert, C. H., & Robinson, M. S. 2018, Lunar Science Targets for Landed Missions (Moffett Field, CA: NASA), LLW2018
Weiss, B. P., & Tikoo, S. M. 2014, Sci, 346, 1198
Whitaker, E. A. 1972, Apollo 15 Preliminary Science Report (Washington, DC: USGO), 25
Wieczorek, M. A., Jolliff, B. A., Khan, A., et al. 2006, RvMG, 60, 221
Wilson, L., & Head, J. W. 2017a, Icar, 283, 146
Wilson, L., & Head, J. W. 2017b, JVGR, 335, 113
Wilson, L., & Head, J. W. 2018, GeoRL, 45, 5852
Wilson, L., & Head, J. W., III 1981, JGR, 86, 2971
Wilson, L., & Head, J. W., III 1988, JGR, 93, 14785
Xiao, L., Zhu, P., Fang, G., et al. 2015, Sci, 347, 1226
Xiao, Y., Su, Y., Dai, S., et al. 2019, AdSpR, 63, 3404
Zanetti, M., Stadermann, A., Jolliff, B., et al. 2017, Icar, 298, 64
Zhang, F., Zhu, M. H., Bugiolacchi, R., et al. 2018, Icar, 307, 216
Ziethe, R., Seiferlin, K., & Hiesinger, H. 2009, P&SS, 57, 784